Common Genetic Variants Influence Whorls in Fingerprint Patterns

TO THE EDITOR

Early work on dermatoglyphics identified three major categories of fingerprint patterns: arches, whorls, and loops, differentiated according to landmark structures formed by the triradii and core (Holt, 1968). These pattern formations are determined by the ratio of volar pad height to width in utero (Mulvihill and Smith, 1969) influenced by genetic interactions with the intrauterine environment (Penrose, 1968). Mathematical models suggested for dermatoglyphic development include heterogeneous genetic factors suggestive of a morphogenetic field effect (Martin et al., 1982). Multivariate linkage analyses revealed a pattern of factor loadings for ridge count that supported this argument and found linkage to 5q14.1 driven by the index, middle, and ring fingers (Medland et al., 2007a). A very high heritability ($h^2 = 0.65$–0.96) has been reported for dermatoglyphic characteristics (Machado et al., 2010), suggesting a genetic basis for pattern type. Building on these previous findings, the present study sought to identify genetic variants associated with fingerprint patterns on each digit using data from the Queensland Institute of Medical Research (QIMR) twin studies and from the Avon Longitudinal Study of Parents and Children (ALSPAC) birth cohort study (Boyd et al., 2013). Participants and their parents (where applicable) provided written informed consent, and ethical approval was obtained from the ALSPAC Ethics and Law committee and the Local Research Ethics Committees.

The QIMR cohort comprised 3,301 participants from 1,764 families. Fingerprints were collected using rolled ink prints on paper, and or using an electronic rolled fingerprint scanner (Smiths Heimann Biometrics ACCO1394) (Medland et al., 2007b). Pattern intensity (the number of triradii) were then manually coded (by SEM and DZL). Within the ALSPAC cohort, 5,339 individuals had genome-wide genotyping and finger pattern information (the study website contains details of data available through a fully searchable data dictionary: http://www.bris.ac.uk/alspac/researchers/data-access/data-dictionary/). Pattern type for each digit was scored and coded (by SEM) from photocopies of the palmar surface of the hands (Medland et al., 2010). Any digit for which the fingerprint pattern was not clearly visible was coded as missing. Because the full patterns of the thumbs were not clearly visible, this digit from excluded from analyses. Intensity and ridge count data were then recoded in terms of presence or absence of whorls and arches on each digit, with loops as the reference category because they are the most common pattern type. Arches were not analyzed because of low pattern frequency. For reference, the thumb on each hand was coded 1 and the little finger as 5, and the right or left hand was designated using the prefix R or L. After quality control, 10 variables were included in the study: presence of whorls across all digits (L1–5, R1–5) L1 and R1 were unavailable for the ALSPAC cohort and L4, L5, R4, and R5 for the QIMR adult sample.

Both QIMR and ALSPAC samples were imputed using the Hapmap2 r22.36 CEU reference. Single nucleotide polymorphisms (SNPs) that had a minor allele frequency >.01 and could be imputed with confidence ($R^2 > 0.3$) were used in these analyses. Only genotyped SNPs were used for chromosome X.

Heritability estimates were obtained from the QIMR data using OpenMX (Boker et al., 2012) (see Supplementary Table S1 online). Principal components analysis was performed with Varimax rotation to investigate latent factors within phenotypes after orthogonal transformation of correlations. Results showed three underlying components of pattern type: whorls on the middle three fingers (digits 2, 3, and 4) on both hands, whorls on the thumbs (digit 1), and whorls on the little fingers (digit 5) (see Supplementary Table S2 online).

Genome-wide analyses were conducted using merlin-offline (QIMR) or Mach2dat (ALSPAC) (Abecasis et al., 2002), for each digit in each cohort and combined using Stouffer's Z score method in METAL to calculate meta-analytic *P*-values (Willer and Abecasis, 2010). There was no evidence of systematic inflation in the QIMR ($\lambda = 1.004$–1.027) or ALSPAC ($\lambda = 1.007$–1.034) results (see Supplementary Figures S1–S3 online). Several genome-wide significant SNPs were found ($P < 5 \times 10^{-8}$). Univariate GWAS for the QIMR sample yielded genome-wide significant *P*-values for rs1523452 ($P = 7.12 \times 10^{-9}$) and for adjacent SNPs rs 2244503 ($P = 1.52 \times 10^{-8}$), rs796973 ($P = 5.47 \times 10^{-8}$), and rs17071864 ($P = 5.42 \times 10^{-8}$) for the WL5 phenotype (see Supplementary Table S3 online). These were independently replicated in the ALSPAC sample (rs1523452, $P = 1.60 \times 10^{-20}$; rs2244503, $P = 3.76 \times 10^{-19}$; rs796973, $P = 2.15 \times 10^{-20}$; rs17071864, $P = 5.68 \times 10^{-20}$) and are encompassed by a single gene *ADAMTS9-AS2* (see Supplementary Figure S4 online). These signals were strengthened in meta-analysis (Figure 1). SNPs within a 2-kbp intergenic region downstream of *TBX3* and upstream of *MED13L* within chr12 were also genome-wide significant for WL4 and WR4, peaking at rs1863718 ($P = 8.04 \times 10^{-9}$ and 1.36×10^{-8}, respectively), and a variant within the *OLA1* gene region was significant for
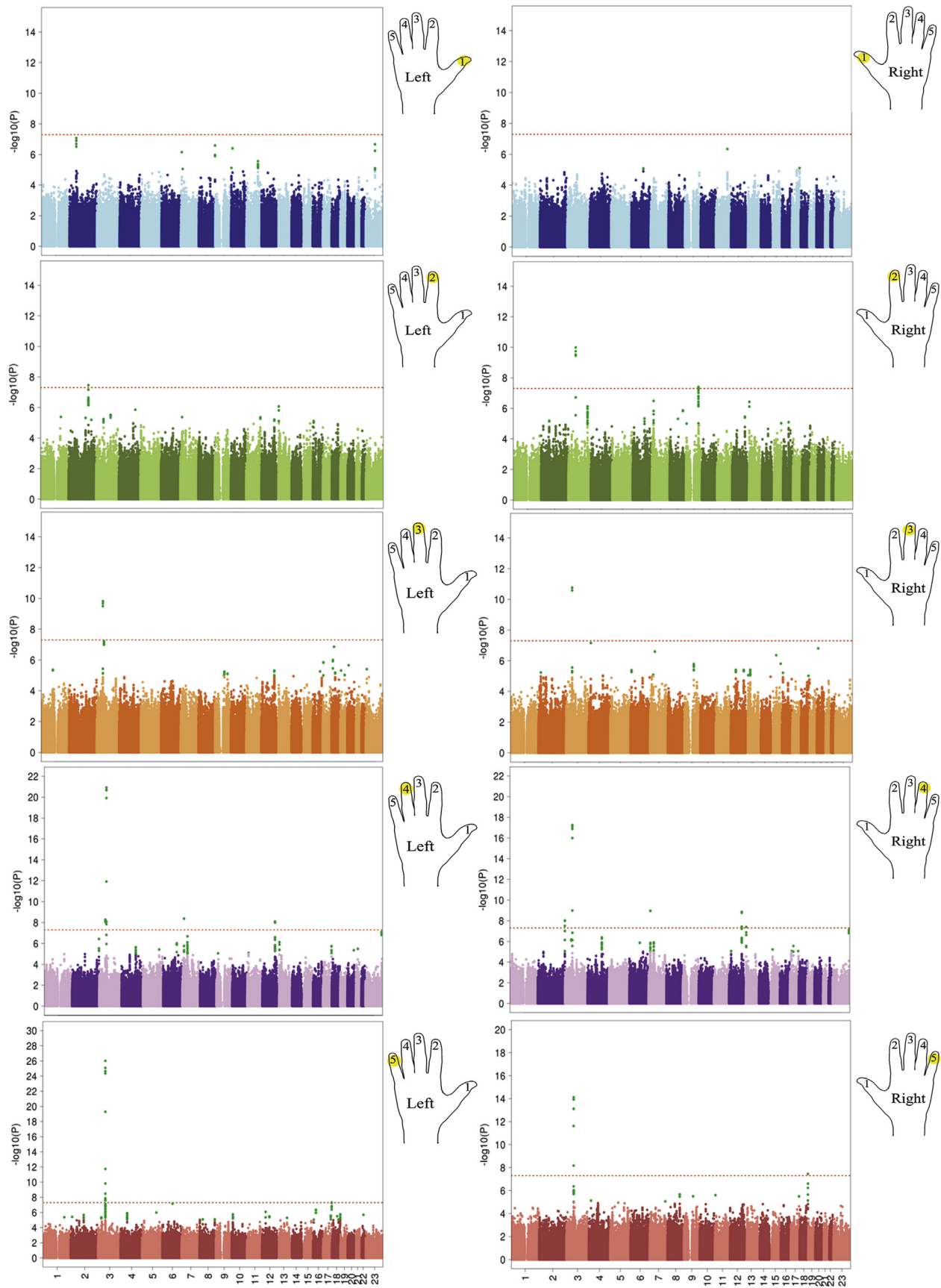
Figure 1. Manhattan plots for meta-analysis results. rs1523452 within the ADAMTS9-AS2 gene region presented the strongest signal for phenotypes WL5 ($P = 9.74 \times 10^{-27}$) and WR5 ($P = 7.62 \times 10^{-15}$), accounting for 1.61% and 0.93% of the variance. rs1523452 also influences WL4 ($P = 2.16 \times 10^{-21}$), WR4 ($P = 1.33 \times 10^{-17}$), and WR2 ($P = 3.08 \times 10^{-10}$), attenuating at WL2 ($P = 9.24 \times 10^{-6}$) and further reduced for WL1 ($P = 2.66 \times 10^{-5}$) and WR1 ($P = 0.0001$).
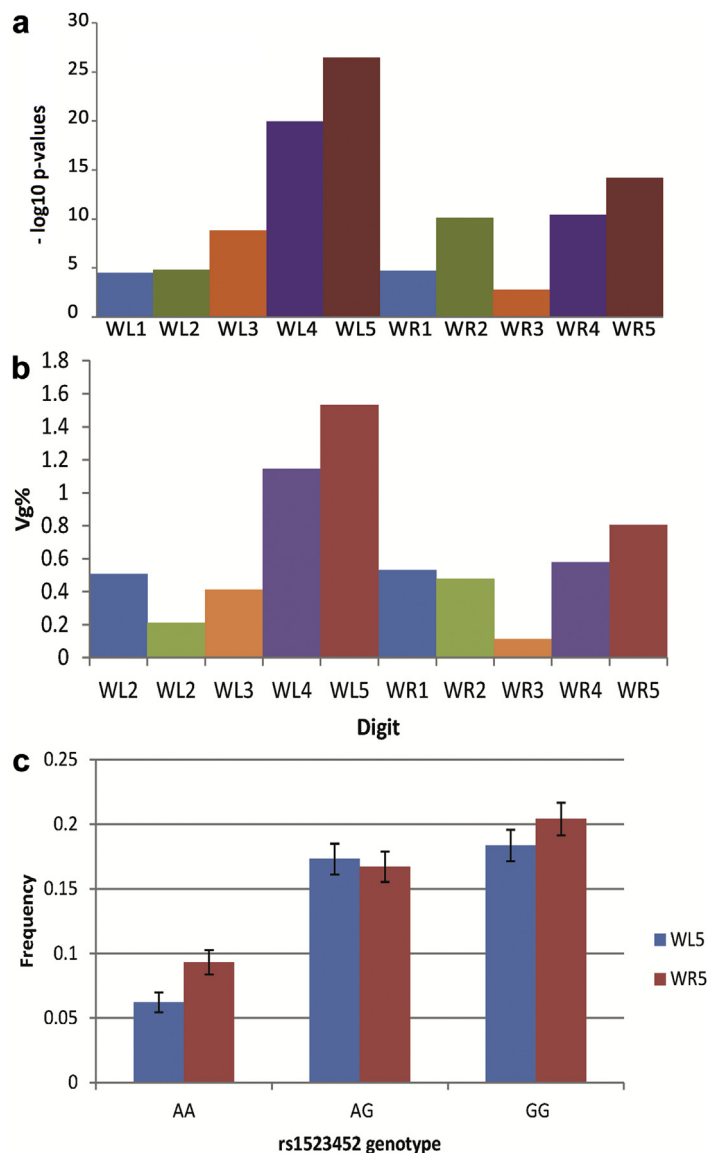
Figure 2. Histograms of meta-analyses results. (**a**) −log10 (*P*-values) and (**b**) percent variation explained by rs1523452 (within the ADAMTS9-AS2 gene region) across digits, obtained by $Z^2/(N-2+Z^2)$. (**c**) Trait frequency as a function of allelic variation. Frequency of whorls on the left little finger (WL5; blue bars) and right little finger (WR5; red bars) as a function of the genotype rs1523452 in a sample of unrelated individuals from the QIMR$_1$ cohort (n[AA] = 708, n[AG] = 335, n[GG] = 49). With more G alleles, the proportion of whorls increases. Vertical bars correspond to the 95% confidence intervals on prevalence.

WL2 (rs10201863, $P = 3.46 \times 10^{-8}$). To further explore variants at the gene level, gene-based tests were conducted using GATES procedure in KGG2.5 (see Supplementary Table S4 online) (Li et al., 2011).

ADAMTS9-AS2 and OLA1 are documented oncogenes down-regulated in glioma (Yao et al., 2014). They are also involved in the inhibition of in vitro cell migration of breast cancer cell lines (Zhang et al., 2009). The associations observed on chromosome 12 between 113904923 and 113903069 bp are located in an intergenic region close to *TBX3,* which is a known cause of ulnar mammary syndrome. This finding concurs with previous literature that limb development in utero influences subsequent fingerprint patterns that emerge (Mulvihill and Smith, 1969).

ADAMTS9-AS2 is an antisense RNA located at 3p14.1, which may be an mRNA inhibitor for the adjacent gene ADAMTS9. Although there is no direct explanation for the role of ADAMTS9-AS2 in the development of whorls on the little fingers, RNA sequencing shows high expression in reproductive organs as well as in the colon and lungs,

suggesting it may be influential in early organ development. *ADAMTS9* and *OLA1* are also expressed in low to medium levels in the skin. Interestingly, variants in *ADAMTS9-AS2* appear to influence whorls on all digits to differing levels (Figure 2a and b) consistent with the hypothesis of a morphogenic field. Allele frequencies at this variant show that the G allele was associated with a higher incidence of whorls (Figure 2c).

Although this study did not find direct evidence for the effects of single genetic variants on specific fingerprint pattern phenotypes, variants within *ADAMTS9-AS2* show a gradient influence on whorls across all digits.

Yvonne Y.W. Ho[1,2,*]
David M. Evans[3,4,*],
Grant W. Montgomery[1],
Anjali K. Henders[1], John P. Kemp[3,4],
Nicholas J. Timpson[3]
Beate St. Pourcain[5,6],
Andrew C. Heath[7],
Pamela A.F. Madden[7],
Danuta Z. Loesch[8], Dennis McNevin[9],
Runa Daniel[10], George Davey-Smith[3],

**Nicholas G. Martin[1] and
Sarah E. Medland[1]**

[1]QIMR Berghofer Medical Research Institute,
Brisbane, Australia; [2]School of Psychology,
University of Queensland, Brisbane, Australia;
[3]MRC Integrative Epidemiology Unit, School of
Social and Community Medicine, University of
Bristol, Bristol, UK; [4]University of Queensland
Diamantina Institute, Translational Research
Institute, Brisbane, Australia; [5]School of Social
& Community Medicine, University of Bristol,
Oakfield House, Oakfield Grove, Bristol, UK;
[6]Max Planck Institute for Psycholinguistics,
Nijmegen, The Netherlands; [7]Department of
Psychiatry, Washington University, St. Louis,
Missouri, USA; [8]Department of Psychology, La
Trobe University, Melbourne, Australia;
[9]National Centre for Forensic Studies, Faculty
of Engineering, Science, Technology and
Mathematics, University of Canberra,
Canberra, Australia; and [10]Office of the Chief
Forensic Scientist, Forensic Services
Department, Victoria Police, Australia
[*]Corresponding author e-mail: Yvonne.Ho@
qimrberghofer.edu.au or d.evans1@uq.edu.au

SUPPLEMENTARY MATERIAL

Supplementary material is linked to the online version of the paper at www.jidonline.org, and at http://dx.doi.org/10.1016/j.jid.2015.10.062.

REFERENCES

Abecasis GR, Cherny SS, Cookson WO, et al. Merlin-rapid analysis of dense genetic maps using sparse gene flow trees. Nat Genet 2002; 30:97−101.

Boker S, Neale M, Maes H, et al. OpenMx 1.2 User Guide. Charlottesville, VA: Department of Psychology, University of Virginia; 2012.

Boyd A, Golding J, Macleod J, et al. Cohort profile: the "children of the 90s"—the index offspring of the Avon Longitudinal Study of Parents and Children. Int J Epidemiol 2013;42: 111−27.

Holt S. The genetics of dermal ridges. Springfield, IL: Charles C. Thomas; 1968.

Li M, Gui H, Kwan J, et al. GATES: a rapid and powerful gene-based association test using extended Simes procedure. Am J Hum Genet 2011;88:283−93.

Machado J, Fernandes P, Roquetti R, et al. Digital dermatoglyphic heritability differences as evidenced by a female twin study. Twin Res Hum Genet 2010;13:482−9.

Martin N, Eaves L, Loesch D. A genetical analysis of covariation between finger ridge counts. Ann Hum Biol 1982;9:539−52.

Medland S, Loesch D, Mdzewski B, et al. Linkage analysis of a model quantitative trait in humans: finger ridge count shows significant multivariate

linkage to 5q14.1. PLoS Genet 2007a;3: 1736−44.

Medland S, Park D, Loesch D, et al. Ridgecounter: a program for obtaining semi-automated finger ridge counts. Ann Hum Biol 2007b;34: 504−17.

Medland S, Zayats T, Glaser B, et al. A variant in LIN28B is associated with 2D:4D finger-length ratio, a putative retrospective biomarker of prenatal testosterone exposure. Am J Hum Genet 2010;86:519−25.

Mulvihill J, Smith D. The genesis of dermatoglyphics. J Pediatr 1969;75:579−89.

Penrose L. Memorandum on dermatoglyphic nomenclature, Birth Defects Original Article Series, vol. 4. NY: National Foundation-March of Dimes; 1968.

Willer C, Li Y, Abecasis G. METAL: fast and efficient meta-analysis of genomewide association scans. Bioinformatics 2010;26: 2190−1.

Yao J, Zhou B, Zhang J, et al. A new tumor suppressor LncRNA ADAMTS9-AS2 is regulated by DNMT1 and inhibits migration of glioma cells. Tumour Biol 2014;35:1−10.

Zhang J, Rubio V, Zheng S, et al. Knockdown of OLA1, a regulator of oxidative stress response, inhibits motility and invasion of breast cancer cells. J Zhejiang Univ Sci B 2009;10:796−804.

Bacterial Sepsis Increases Survival in Metastatic Melanoma: *Chlamydophila Pneumoniae* Induces Macrophage Polarization and Tumor Regression

CrossMark

TO THE EDITOR

The initiative of this study was the unexpected complete tumor regression in a patient with stage IV cutaneous metastatic melanoma, who suffered multifactorial sepsis syndrome during BOLD (bleomycin, oncovin, lomustine, and dacarbazine) chemotherapy (see Supplementary Figure S1 online). After targeted antibiotic treatment and combined complication-free chemotherapy, the patient's physical condition improved, and the metastases

unexpectedly disappeared. The patient has been asymptomatic and metastasis-free since the end of BOLD therapy. A significant decrease in the volume of the previously palpable axillary and abdominal metastases had already been observed when BOLD therapy was interrupted because of sepsis. A timeline of events is given in Table 1.

Molecular genetics research in the last decade assisted in the development of BRAF inhibitors and immuno-oncological agents, which resulted in

significant improvement in the life expectancy of melanoma patients. Dacarbazine-based chemotherapies, once the gold standard (Hobohm, 2001; Wiemann and Starnes, 1994), are still approved and widely applied in melanoma therapy, but their efficacy is relatively low (Garbe et al., 2011). Therefore, the fact that clinical improvement was observed quite early during the chemotherapy suggested other factors behind the outcome, and the concurrent sepsis seemed to offer a potential explanation.

It has long been recognized that cancer patients might recover after bacterial infections (Hobohm, 2001). The hypothesis was that fever and tumor necrosis factor-α induced by the

---